Supplementary Information

Two Novel Rab2 Interactors Regulate Dense-core Vesicle Maturation

Michael Ailion, Mandy Hannemann, Susan Dalton, Andrea Pappas, Shigeki Watanabe, Jan Hegermann, Qiang Liu, Hsiao-Fen Han, Mingyu Gu, Morgan Q. Goulding, Nikhil Sasidharan, Kim Schuske, Patrick Hullett, Stefan Eimer, and Erik M. Jorgensen

RUND-1 alignment

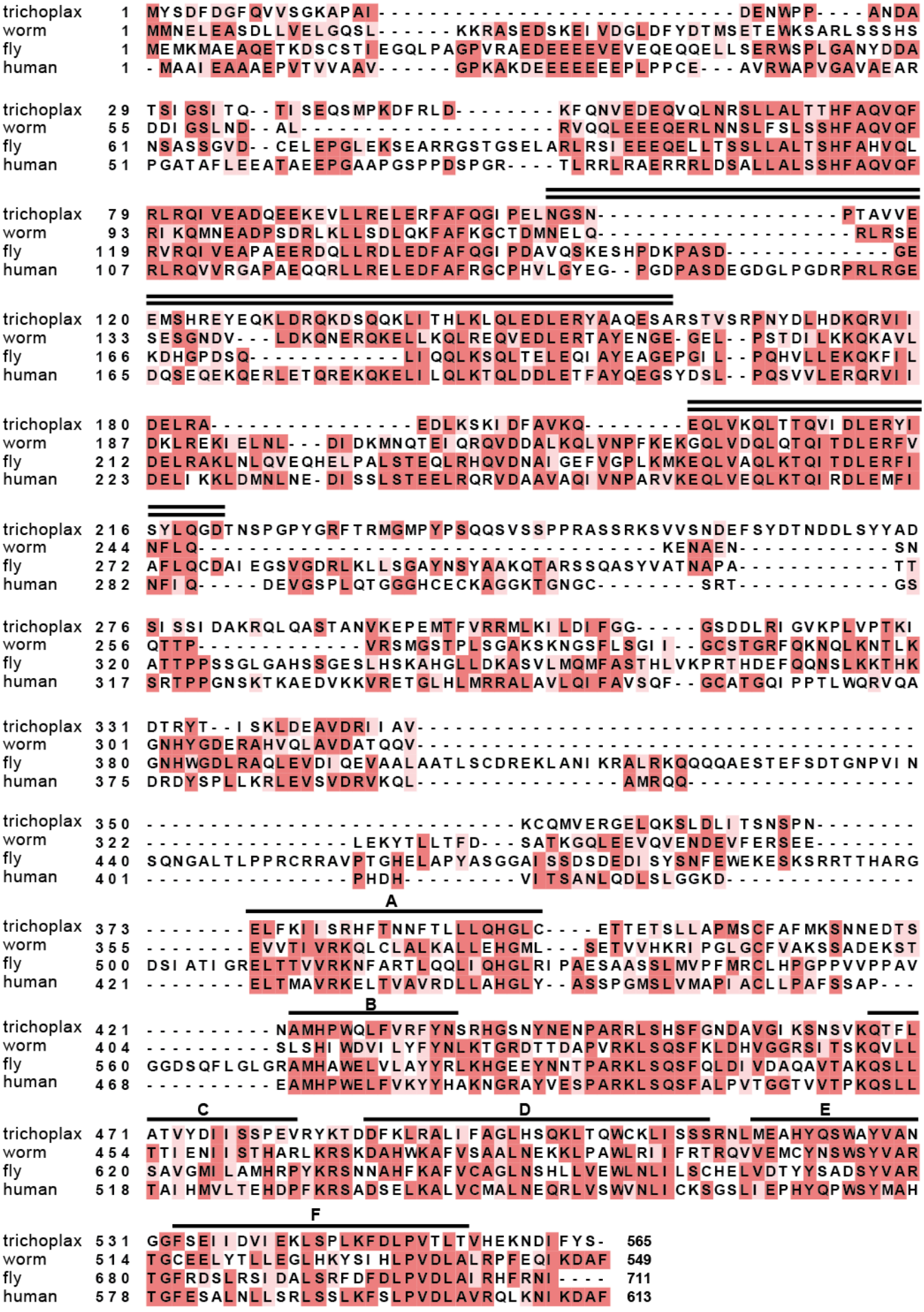

CCCP-1 alignment

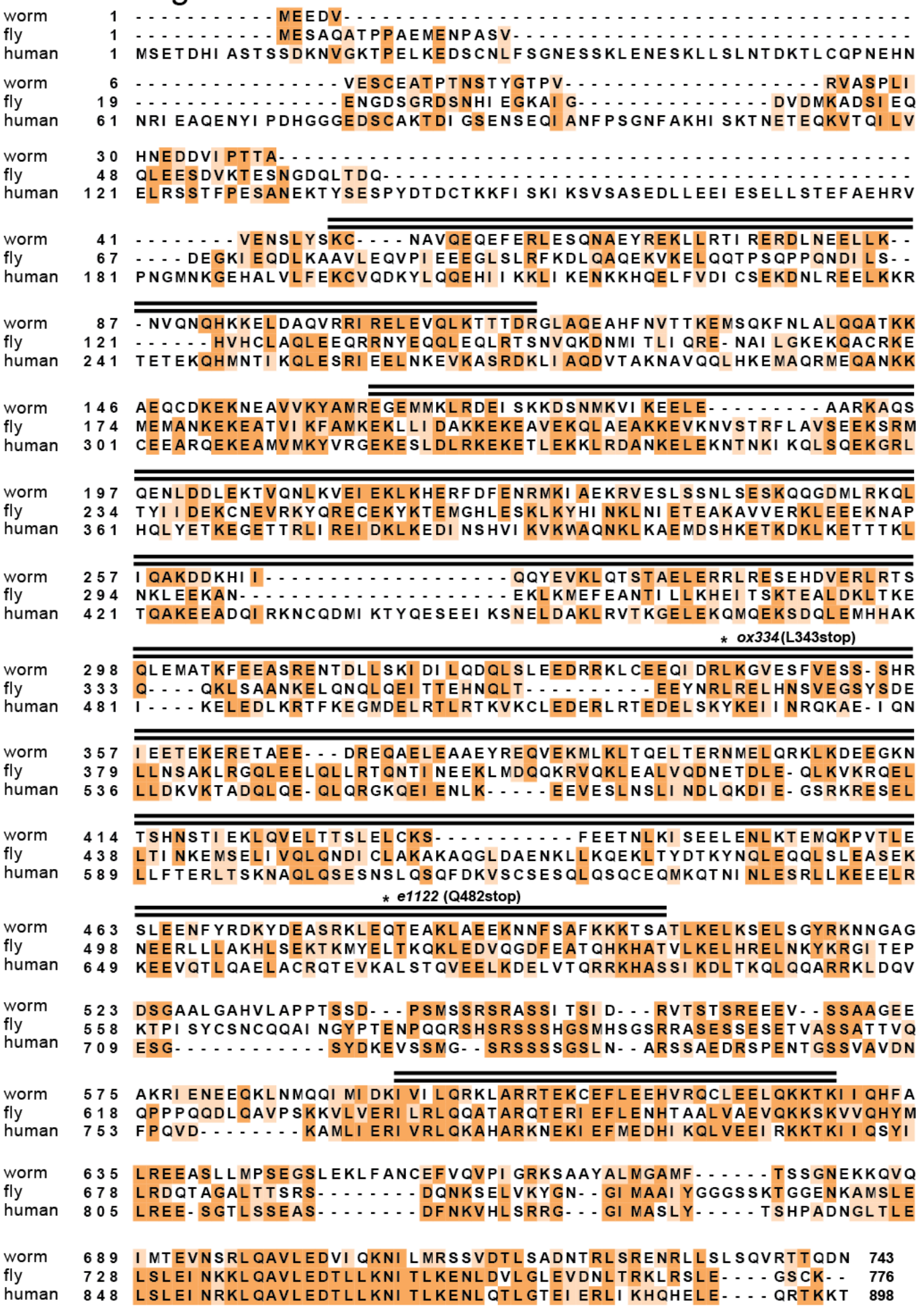

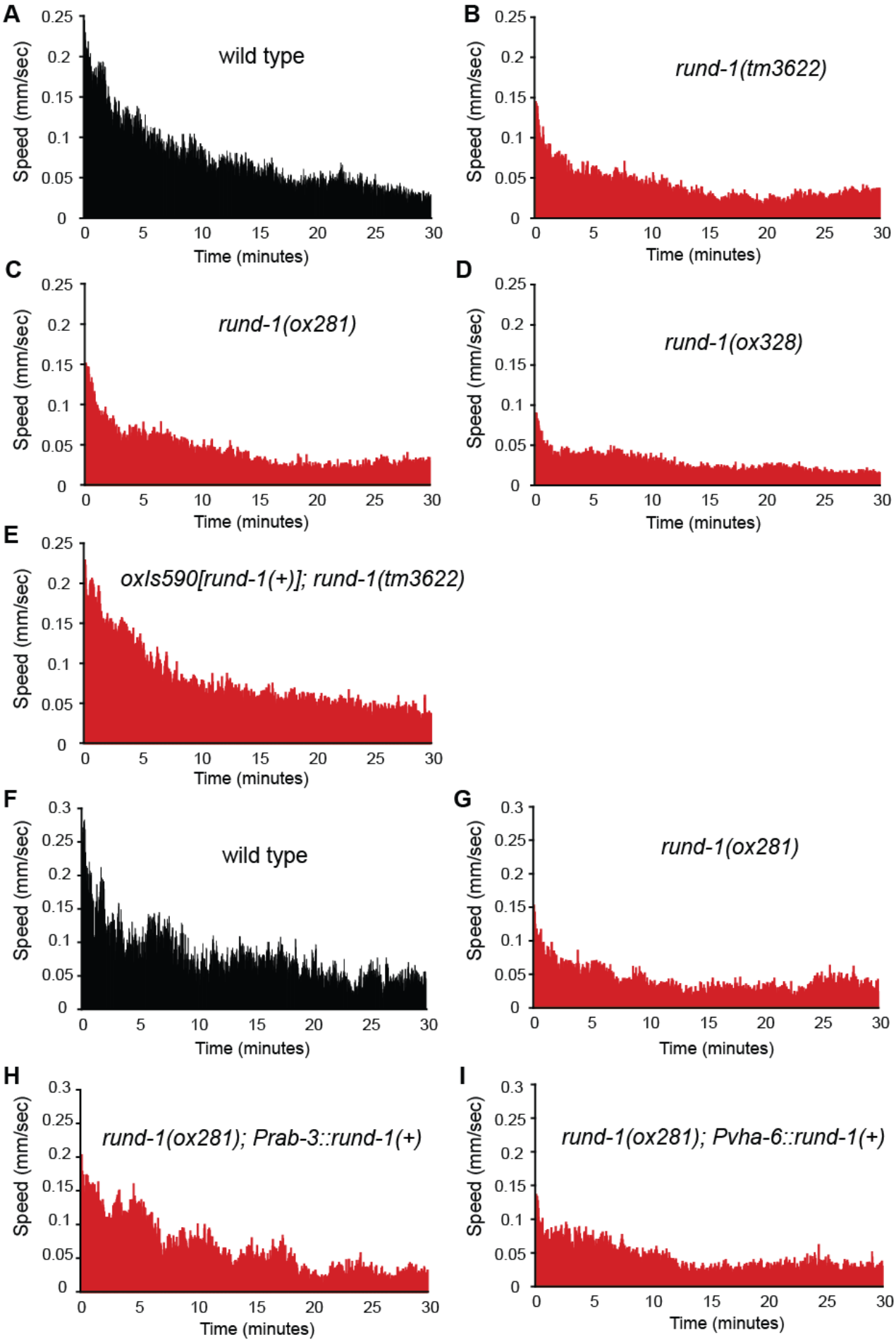
A
wild type
B
rund-1(tm3622)
C
rund-1(ox281)
D
rund-1(ox328)
E
oxIs590[rund-1(+)]; rund-1(tm3622)
F
wild type
G
rund-1(ox281)
H
rund-1(ox281); Prab-3::rund-1(+)
I
rund-1(ox281); Pvha-6::rund-1(+)
Speed (mm/sec)
Time (minutes)

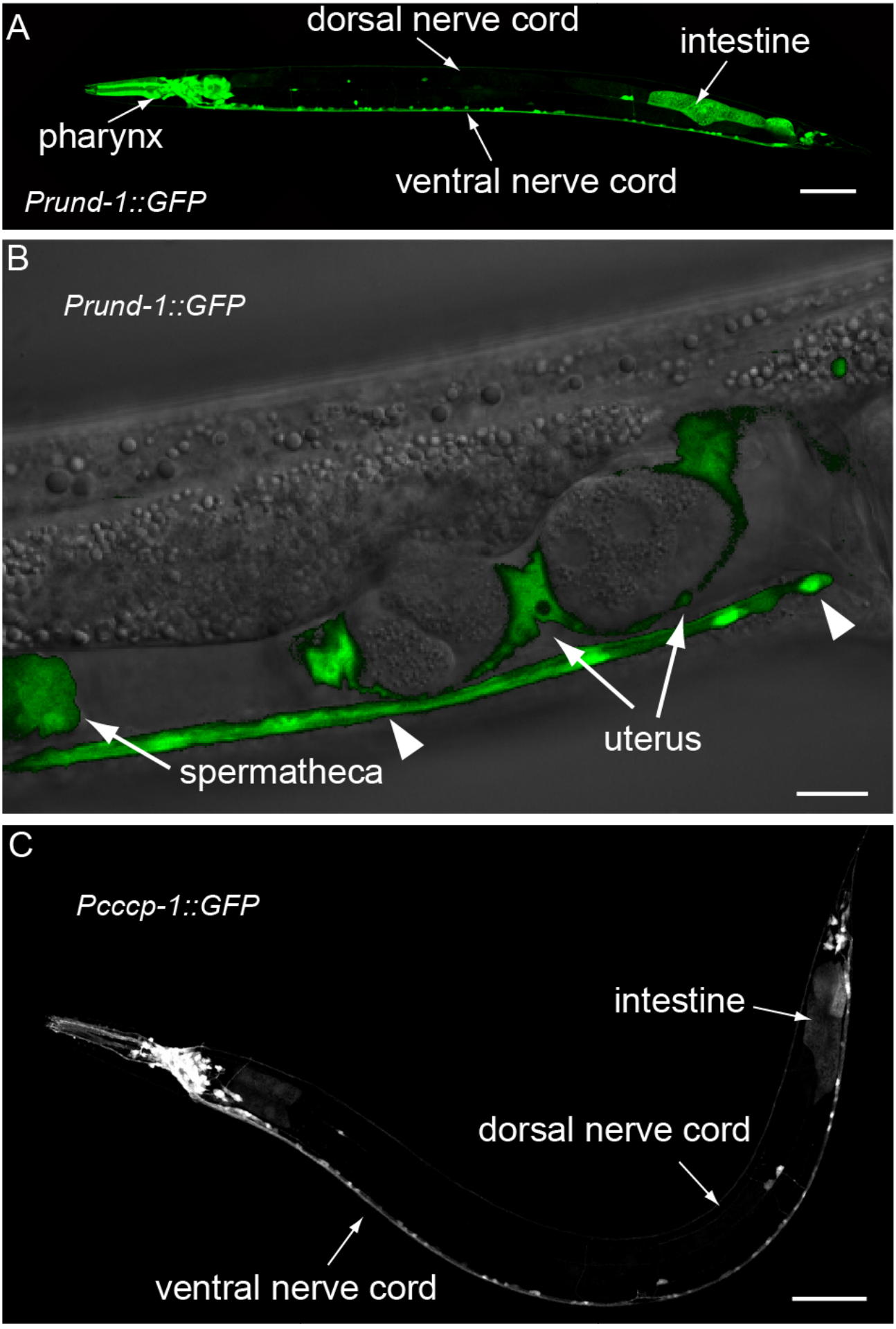
A
dorsal nerve cord
intestine
pharynx
ventral nerve cord
Prund-1::GFP
B
Prund-1::GFP
uterus
spermatheca
C
Pcccp-1::GFP
intestine
dorsal nerve cord
ventral nerve cord

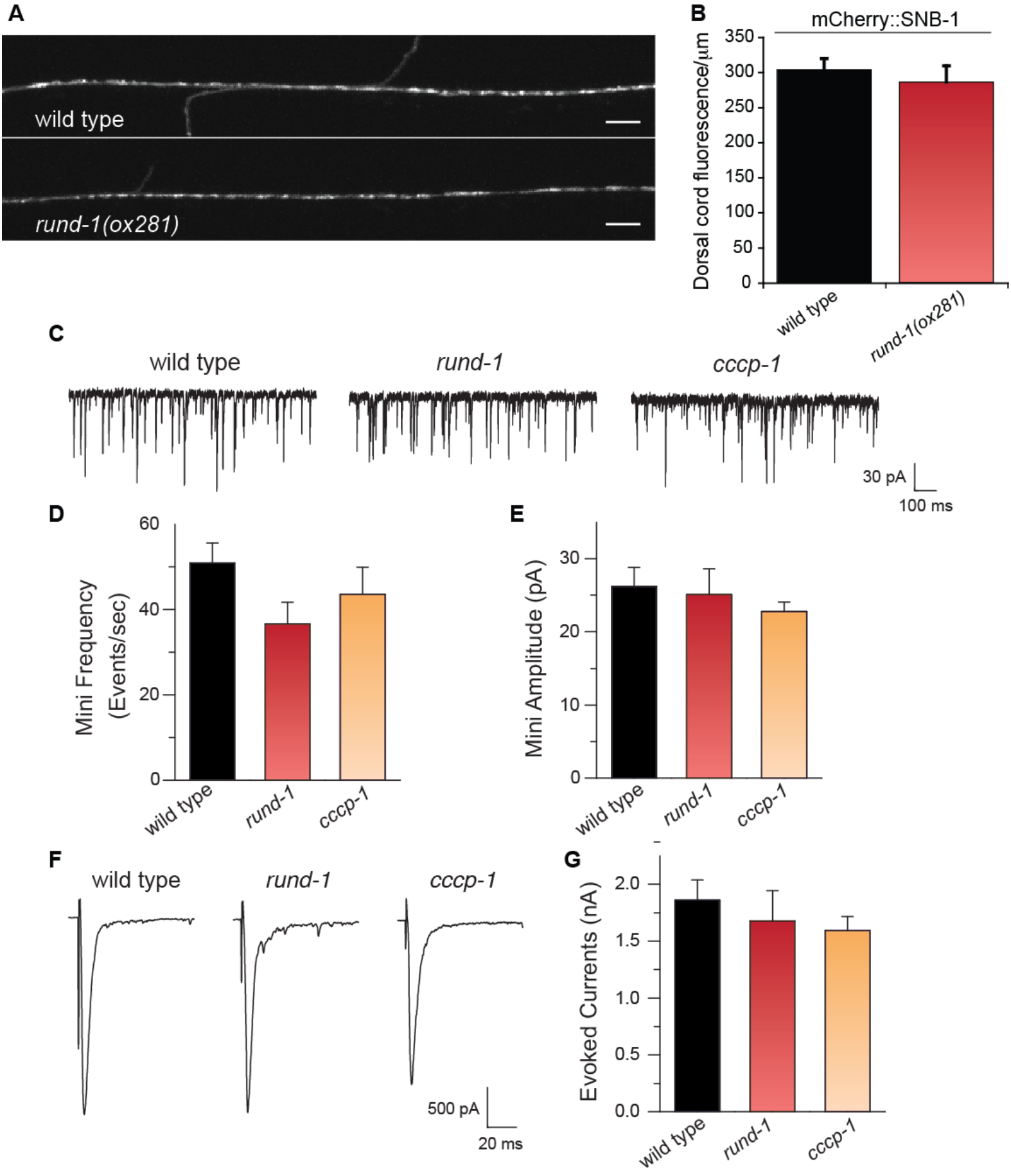
A
wild type
rund-1(ox281)
B
mCherry::SNB-1
Dorsal cord fluorescence/µm
350
300
250
200
150
100
50
0
wild type
rund-1(ox281)
C
wild type
rund-1
cccp-1
30 pA
100 ms
D
Mini Frequency (Events/sec)
60
40
20
0
wild type
rund-1
cccp-1
E
Mini Amplitude (pA)
30
20
10
0
wild type
rund-1
cccp-1
F
wild type
rund-1
cccp-1
500 pA
20 ms
G
Evoked Currents (nA)
2.0
1.5
1.0
0.5
0.0
wild type
rund-1
cccp-1

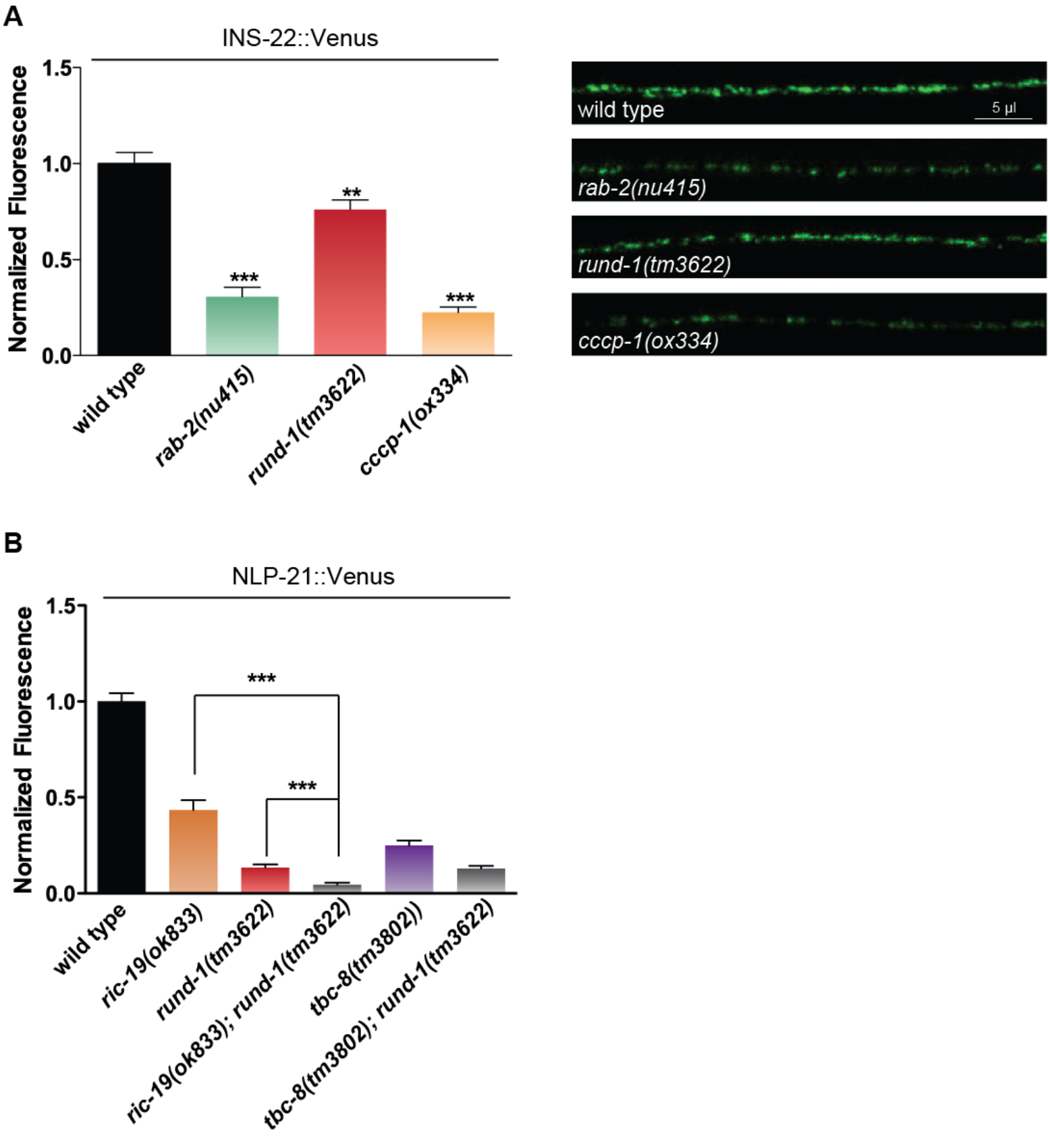
A
INS-22::Venus
Normalized Fluorescence
1.5
1.0
0.5
0.0
**
***
***
wild type
rab-2(nu415)
rund-1(tm3622)
cccp-1(ox334)
wild type
5 µl
rab-2(nu415)
rund-1(tm3622)
cccp-1(ox334)
B
NLP-21::Venus
Normalized Fluorescence
1.5
1.0
0.5
0.0
***
***
wild type
ric-19(ok833)
rund-1(tm3622)
ric-19(ok833); rund-1(tm3622)
tbc-8(tm3802))
tbc-8(tm3802); rund-1(tm3622)

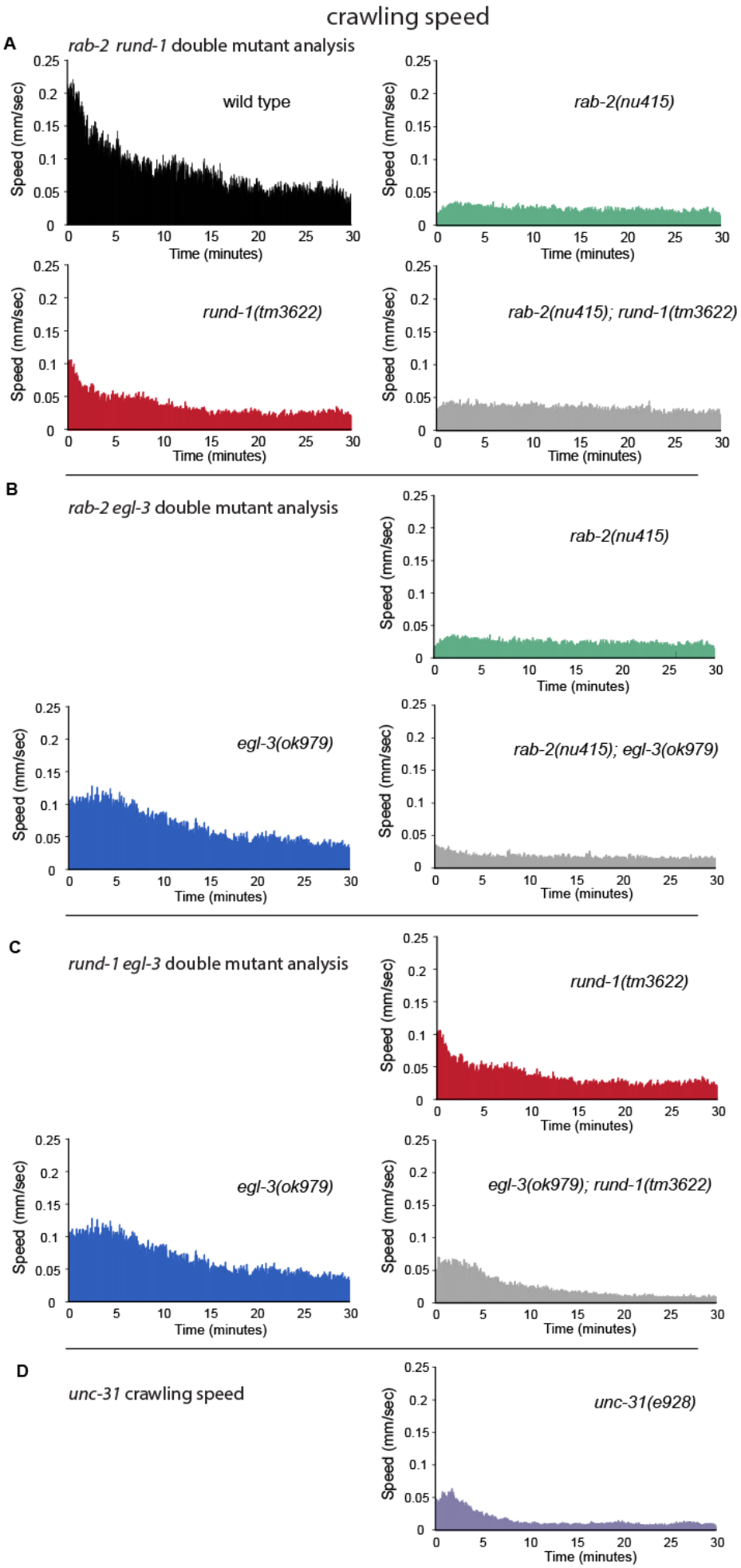
crawling speed
A
rab-2 rund-1 double mutant analysis
wild type
rab-2(nu415)
rund-1(tm3622)
rab-2(nu415); rund-1(tm3622)
B
rab-2 egl-3 double mutant analysis
rab-2(nu415)
egl-3(ok979)
rab-2(nu415); egl-3(ok979)
C
rund-1 egl-3 double mutant analysis
rund-1(tm3622)
egl-3(ok979)
egl-3(ok979); rund-1(tm3622)
D
unc-31 crawling speed
unc-31(e928)
Speed (mm/sec)
Time (minutes)
0
0.05
0.1
0.15
0.2
0.25
0
5
10
15
20
25
30

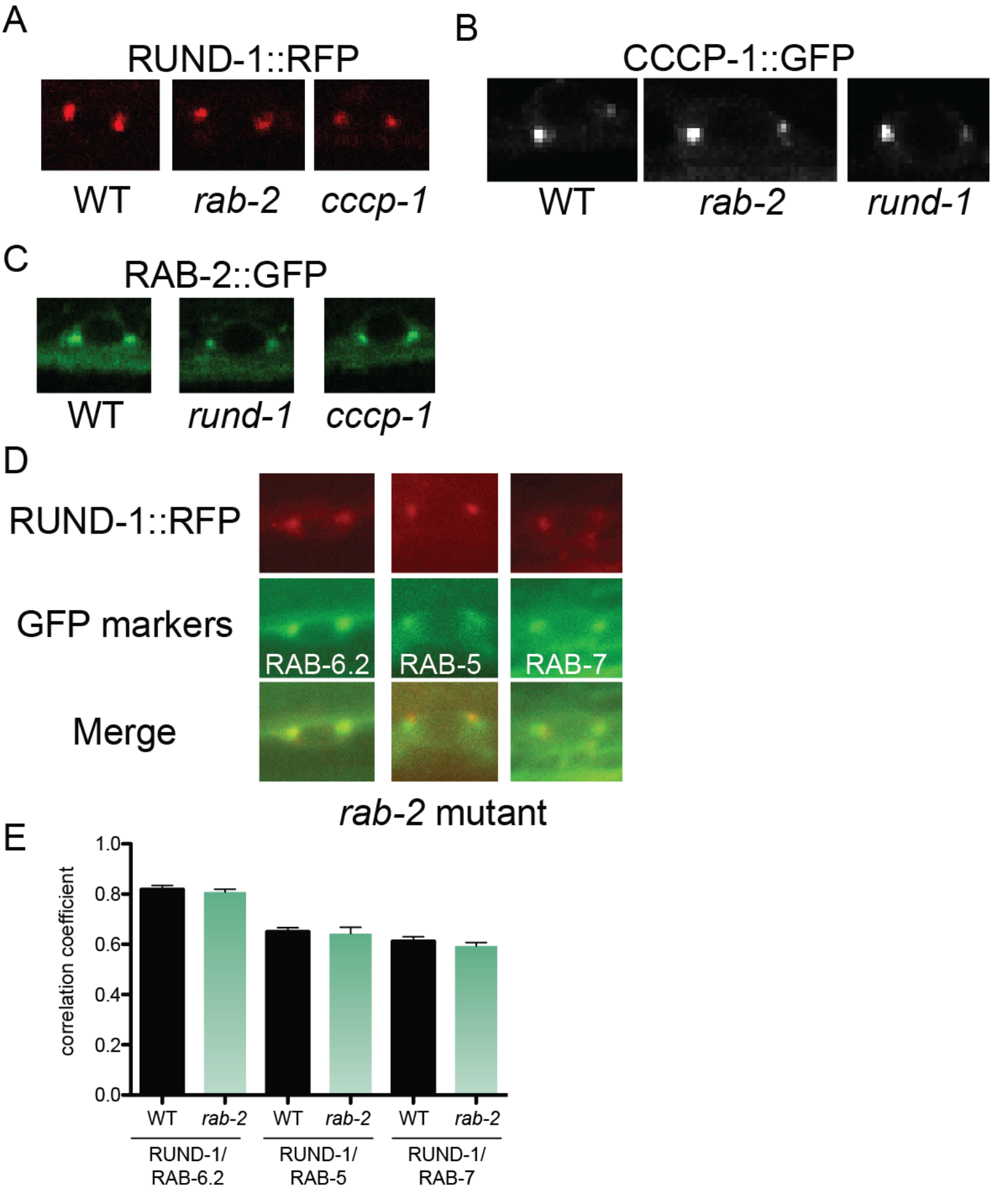
A
RUND-1::RFP
WT
rab-2
cccp-1
B
CCCP-1::GFP
WT
rab-2
rund-1
C
RAB-2::GFP
WT
rund-1
cccp-1
D
RUND-1::RFP
GFP markers
Merge
RAB-6.2
RAB-5
RAB-7
rab-2 mutant
E
correlation coefficient
1.0
0.8
0.6
0.4
0.2
0.0
WT
rab-2
WT
rab-2
WT
rab-2
RUND-1/ RAB-6.2
RUND-1/ RAB-5
RUND-1/ RAB-7

Supplemental Information

Supplemental Figure and Movie Legends

Figure S1. Alignment of the full-length RUND-1 protein. (related to Figure 1)
Alignment of *C. elegans* RUND-1 (worm, accession # JN986879) and its orthologs from *Trichoplax adhaerens* (Trichoplax, hypothetical protein TRIADDRAFT_52054, accession # XP_002108010.1), *Drosophila melanogaster* (fly, CG3703, accession # NP_569874.1) and *Homo sapiens* (human, RUNDC1, accession # AAH39247.1). Identical residues are shaded in darker red and similar residues are shaded in lighter red. The coiled-coil domains (from SMART, using the worm protein; http://smart.embl-heidelberg.de/) are marked with double black bars. The six conserved blocks A-F of the RUN domain (Callebaut et al., 2001) are marked with single black bars. Alignment was made with MUSCLE (Edgar, 2004) using default parameters and exhibited with Boxshade 3.21 (http://www.ch.embnet.org/software/BOX_form.html).

Figure S2. Alignment of the full-length CCCP-1b protein. (related to Figure 1)
Alignment of *C. elegans* CCCP-1b (worm, accession # JN986880) and its orthologs from *Drosophila melanogaster* (fly, CG4925, accession # NP_648879.1) and *Homo sapiens* (human, C10orf118, accession # AAI03500.1). Identical residues are shaded in darker yellow and similar residues are shaded in lighter yellow. The coiled-coil domains (from SMART, using the worm protein; http://smart.embl-heidelberg.de/) are marked with double black bars. The positions of the *ox334* and *e1122* stop mutations are marked with asterisks. Alignment was made with MUSCLE (Edgar, 2004) using default parameters and exhibited with Boxshade 3.21 (http://www.ch.embnet.org/software/BOX_form.html).

Figure S3. Locomotion data. (related to Figure 2)
(A-E) Each graph shows the mean speed of 21 to 27 animals during the 30 minute period immediately after being transferred to a new plate. These graphs show the complete tracking data associated with the left side of Figure 2C.
(F-I) Each graph shows the mean speed of 9 animals during the 30 minute period immediately after being transferred to a new plate. These graphs show the complete tracking data associated with the right side of Figure 2C.

Figure S4. *rund-1* and *cccp-1* are expressed widely in neurons and other tissues.
Expression of *rund-1* and *cccp-1* promoter::GFP fusions are shown in transgenic animals carrying extrachromosomal arrays.
(A) An L4 stage late-larval animal is shown. *Prund-1::GFP* is expressed throughout the nervous system, including head and tail neurons and motor neurons in the ventral cord. Expression is also observed in the pharynx and intestine, but not in skin or muscle cells. This animal has intestinal expression in only the posterior intestine due to mosaicism of the extrachromosomal array. Scale bar: 50 μm.
(B) Expression of *Prund-1::GFP* in the spermatheca, uterus and ventral nerve cord (arrowheads) of a gravid adult. GFP and DIC images are superimposed. Scale bar: 10 μm.
(C) An L4 stage late-larval animal is shown. *Pcccp-1::GFP* is expressed throughout the nervous system, including head and tail neurons and motor neurons in the ventral cord. Expression is also seen in the intestine, but is not seen in pharynx, skin or muscle cells. This animal has intestinal expression in only the posterior intestine due to mosaicism of the extrachromosomal array. Scale bar: 50 μm.

Figure S5. *rund-1* and *cccp-1* mutants do not have defects in development or function of synapses.
(A) *rund-1(ox281)* shows normal synaptic development as visualized by *Punc-129::mCherry::snb-1* localization in the dorsal nerve cord of young adult animals. Scale bar: 5 μm.
(B) Quantification of mCherry::SNB-1 fluorescence levels in the dorsal cord. The mean fluorescence intensity per μm is given in arbitrary units. The *rund-1(ox281)* mutant has normal levels of mCherry::SNB-1 in the dorsal cord (P=0.55, two-tailed unpaired t test). Error bars = SEM; n = 6 animals each genotype.
(C) Representative traces of endogenous currents (minis) in wild-type, *rund-1(tm3622)* and *cccp-1(ox334)*.
(D,E) *rund-1* and *cccp-1* mutants have normal mini frequency and amplitude (P>0.05, paired t test). Error bars = SEM; n = 8 animals each genotype.
(F) Representative traces of electrically evoked currents in wild-type, *rund-1(tm3622)* and *cccp-1(ox334)*.
(G) *rund-1* and *cccp-1* mutants have normal evoked currents (P>0.05, paired t test). Error bars = SEM; n = 6-8 animals each genotype.

Figure S6. Dense-core vesicle trafficking phenotypes.
(A) The graph shows quantification of INS-22::Venus fluorescence levels in the dorsal nerve cord. The images show representative examples of the data. *rab-2*, *rund-1*, and *cccp-1* mutants all have decreased trafficking of INS-22::Venus to the dorsal nerve cord (***, P<0.001 compared to wild type; **, P<0.01). Error bars = SEM; n = 18-21 animals each genotype.
(B) *rund-1* and *ric-19* act in parallel. The graph shows quantification of NLP-21::Venus fluorescence levels in the dorsal nerve cord. A *ric-19; rund-1* double mutant has a stronger defect than either a *ric-19* or *rund-1* single mutant (***, P<0.001 for both comparisons). A *tbc-8; rund-1* double mutant does not have a stronger defect than the *rund-1* single mutant (P>0.05). Error bars = SEM; n = 14-70 animals each genotype.

Figure S7. Locomotion data. (related to Figure 2)
Each graph shows the mean speed of 24 to 31 animals during a 30 minute period immediately after being transferred to a new plate. The graphs in panel A show the complete tracking data associated with Figure 2E. Graphs of *rab-2*, *rund-1*, and *egl-3* are repeated in panels A-C for ease of comparison. Though *rab-2* mutants are similar to *rund-1* and *cccp-1* mutants at steady state, *rab-2* mutants are not stimulated by harsh touch like *rund-1*, *cccp-1*, and even *unc-31*/CAPS mutants. The additional lack of stimulated locomotion in *rab-2* mutants may be due to a RAB-2 function that does not require CAPS and thus is likely to be unrelated to dense-core vesicle function.

Figure S8. RUND-1, RAB-2 and CCCP-1 are not required for each other's localization (related to Figure 5)
Each panel shows a single slice of a confocal (A-C) or wide-field (D) image of motor neuron cell bodies in the ventral nerve cord of young adult animals.
(A) RUND-1::RFP is still localized in *rab-2(nu415)* and *cccp-1(ox334)* mutants. The figure shows the expression of the single-copy transgene *oxIs590*.
(B) CCCP-1::GFP is still localized in *rab-2(nu415)* and *rund-1(tm3622)* mutants. The figure shows the expression of the extrachromosomal array *oxEx1366[Pcccp-1::cccp-1(+) cDNA::GFP]*.
(C) GFP::RAB-2 is still localized in *rund-1(tm3622)* and *cccp-1(ox334)* mutants. The figure shows the expression of the single-copy transgene *oxSi314*. GFP is concentrated in puncta in the cell body, but is also seen more diffusely throughout the cell body and the axons.
(D) In a *rab-2(nu415)* mutant, RUND-1::RFP still tightly colocalizes with RAB-6.2, but not with RAB-5 or RAB-7.
(E) RUND-1::RFP tightly colocalizes with RAB-6.2, but not with RAB-5 or RAB-7. The graph shows quantification of colocalization data using the Pearson's correlation coefficient. RUND-1 is

significantly more colocalized with RAB-6.2 than with RAB-5 or RAB-7 ($P<0.0001$, two-tailed unpaired t tests), but no changes in colocalization are seen in a *rab-2* mutant ($P>0.1$ for all three comparisons). Error bars = SEM; n = 10-18 cells each genotype.

Movie S1. Locomotion of the wild-type strain N2, showing normal sinusoidal movement.

Movie S2. Locomotion of the activated Gq mutant *egl-30(tg26)*. *egl-30(tg26)* mutant worms are smaller than wild-type and have hyperactive locomotion with deeper body bends and more frequent reversals.

Movie S3. *rund-1* mutants have unmotivated spontaneous locomotion but respond to touch.
The movie shows a field of *rund-1(ox328)* mutant larval and adult animals on a bacterial lawn. The worms show normal foraging behavior, but little spontaneous locomotion. Beginning at ten seconds into the video, several worms are prodded with a platinum wire worm pick. After being touched, the stimulated worms move away, exhibiting slow but coordinated locomotion.

Movie S4. *rund-1* mutants are stimulated by UV light.
The movie shows a close-up of a single *rund-1(ox328)* adult on a bacterial lawn. It exhibits normal foraging and feeding behavior, but little spontaneous locomotion. At four seconds into the video, UV light is turned on. After a few seconds delay, the worm stops feeding and moves away, exhibiting coordinated locomotion.

Supplemental Tables

Table S1. Rescue of *rund-1* mutants by the human ortholog RUNDC1.

Strain genotype	Animals picked	Presence of array	
		+	-
rund-1(ox281); P*rund-1*::RUNDC1(+)::tagRFP	Unc	0	10
	Non-Unc	10	1
rund-1(tm3622); P*rund-1*::RUNDC1(+)::tagRFP	Unc	1	9
	Non-Unc	11	0

To examine rescue of *rund-1* mutant locomotion by transgenic expression of its human ortholog RUNDC1, approximately ten putative Unc (non-rescued) and Non-Unc (rescued) adult animals were selected from a plate of each strain under a dissecting microscope and subsequently examined for the presence of the extrachromosomal array as scored by fluorescence. The experimenter was blind to the presence of the array at the time the animals were picked. There is strong correlation of the locomotion phenotype to the presence of the array in both strains, indicating that they are rescued (Fisher's Exact Test, two-tailed P value, $P<0.0001$ for both strains).

Table S2. Statistics for locomotion tracking data. (related to Figure 2)

Comparison	Test	P value
N2 vs. *rund-1(tm3622)*	Kruskal-Wallis/Dunn	<0.001
N2 vs. *rund-1(ox281)*	Kruskal-Wallis/Dunn	<0.001
N2 vs. *rund-1(ox328)*	Kruskal-Wallis/Dunn	<0.001
N2 vs. *oxIs590[rund-1(+)]; rund-1(tm3622)*	Kruskal-Wallis/Dunn	>0.05
rund-1(tm3622) vs. *rund-1(ox281)*	Kruskal-Wallis/Dunn	>0.05
rund-1(tm3622) vs. *rund-1(ox328)*	Kruskal-Wallis/Dunn	>0.05
rund-1(tm3622) vs. *oxIs590[rund-1(+)]; rund-1(tm3622)*	Kruskal-Wallis/Dunn	<0.001
rund-1(ox281) vs. *rund-1(ox328)*	Kruskal-Wallis/Dunn	<0.01
N2 vs. *rund-1(ox281); oxEx1197 [Prab-3::rund-1(+)]*	One-way ANOVA/Bonferroni	<0.05
rund-1(ox281) vs. *rund-1(ox281); oxEx1197 [Prab-3::rund-1(+)]*	One-way ANOVA/Bonferroni	<0.01
rund-1(ox281) vs. *rund-1(ox281); oxEx1260 [Pvha-6::rund-1(+)]*	One-way ANOVA/Bonferroni	>0.05
rab-2(nu415) vs. *rund-1(tm3622)*	One-way ANOVA/Bonferroni Kruskal-Wallis/Dunn	<0.001 <0.001
rab-2(nu415) vs. *rab-2(nu415); rund-1(tm3622)*	One-way ANOVA/Bonferroni Kruskal-Wallis/Dunn	>0.05 >0.05
rab-2(nu415) vs. *unc-31(e928)*	One-way ANOVA/Bonferroni Kruskal-Wallis/Dunn	<0.001 <0.01
rab-2(nu415) vs. *egl-3(ok979); rab-2(nu415)*	One-way ANOVA/Bonferroni Kruskal-Wallis/Dunn	>0.05 >0.05
rund-1(tm3622) vs. *rab-2(nu415); rund-1(tm3622)*	One-way ANOVA/Bonferroni Kruskal-Wallis/Dunn	<0.001 <0.001
rund-1(tm3622) vs. *egl-3(ok979); rund-1(tm3622)*	One-way ANOVA/Bonferroni Kruskal-Wallis/Dunn	<0.001 >0.05
egl-3(ok979) vs. *unc-31(e928)*	One-way ANOVA/Bonferroni Kruskal-Wallis/Dunn	<0.001 <0.001
egl-3(ok979) vs. *egl-3(ok979); rab-2(nu415)*	One-way ANOVA/Bonferroni Kruskal-Wallis/Dunn	<0.001 <0.001
egl-3(ok979) vs. *egl-3(ok979); rund-1(tm3622)*	One-way ANOVA/Bonferroni Kruskal-Wallis/Dunn	<0.001 <0.01
unc-31(e928) vs. *egl-3(ok979); rab-2(nu415)*	One-way ANOVA/Bonferroni Kruskal-Wallis/Dunn	<0.001 <0.01
unc-31(e928) vs. *egl-3(ok979); rund-1(tm3622)*	One-way ANOVA/Bonferroni Kruskal-Wallis/Dunn	>0.05 >0.05
egl-3(ok979); rab-2(nu415) vs. *egl-3(ok979); rund-1(tm3622)*	One-way ANOVA/Bonferroni Kruskal-Wallis/Dunn	<0.001 <0.001

Extended Experimental Procedures

Analysis of *rund-1* and *cccp-1* cDNAs

We obtained the *rund-1* cDNA from the ORFeome library, and three predicted full-length SL1 trans-spliced *rund-1* cDNAs from Yuji Kohara. Restriction digests and partial sequencing indicated that all four cDNAs had the same splicing pattern (Figure 1A), with several differences from the gene structure predicted on Wormbase (exon 6 was 174 bp shorter than predicted on Wormbase, and Wormbase exon 7 was not present). The cDNAs yk772b6, yk814f3 and the ORFeome cDNA contained mutations. yk471g7 was sequenced completely and shown to be mutation free. This cDNA was cloned into a Gateway entry vector and used for rescue experiments.

We obtained three *cccp-1* cDNAs from Yuji Kohara. Sequencing revealed two alternatively spliced transcripts, *cccp-1a* (yk812f4) and *cccp-1b* (yk1517a6 and yk530g8), differing in the inclusion of exon 12 (Figure 1A). The existence of both isoforms is supported by additional EST sequences on Wormbase. *cccp-1* is trans-spliced to SL1. cDNAs yk812f4 and yk1517a6 contained mutations. yk530g8 was mutation-free and cloned into a Gateway entry vector for rescue experiments. The full-length sequences of the *rund-1* and *cccp-1b* transcripts were deposited in GenBank under accession numbers JN986879 and JN986880.

Transgenes

A complete list of constructs, including sizes of promoter regions, is provided below. Most of the constructs were made using the three slot multisite Gateway system (Invitrogen). Typically, a promoter, a coding sequence (genomic DNA or cDNA), and an N- or C-terminal fluorescent tag (eGFP or tagRFP-T) were cloned along with a 3'UTR into either pCFJ150 or pCFJ201, destination vectors used for Mos1-mediated single copy insertion (MosSCI) on chromosome II at *ttTi5605* and chromosome IV at *cxTi10882*, respectively (Frøkjaer-Jensen et al., 2008). All insertions were made by the direct injection MosSCI method. For most constructs, we isolated multiple independent insertions that behaved similarly. Extrachromosomal arrays were made by standard transformation methods (Mello et al., 1991).

Yeast two-hybrid assays

The Matchmaker yeast two-hybrid assay was performed according to the manufacturer's protocol (Clontech). *C. elegans rab*, *rap*, *ras*, and *ral* gene cDNAs were cloned into the bait vector pGBKT7, and the *rund-1* and *cccp-1b* cDNAs were cloned into the prey vector pGADT7. The appropriate plasmid combinations were transformed into the yeast strain AH109 and spread onto growth media lacking leucine and tryptophan for plasmid selection. Protein interactions were tested as follows: several clones of transformants were mixed, diluted to an OD_{600} of 0.2 and spotted onto selective plates lacking leucine, tryptophan and histidine. Interactions were identified by growth after three days. All interacting proteins were tested for self-activation by transforming the interacting plasmid with the appropriate empty vector pGBKT7 or pGADT7. Both RUND-1 and RIC-19 self-activated when expressed in the DNA binding domain vector pGBKT7 and thus could not be tested against each other.

Coimmunoprecipitation and immunoblotting

HEK293 cells were grown in high glucose (4.5 g/l) DMEM supplemented with 10% FBS, 110 mg/l sodium pyruvate, 2 mM glutamine, 100 U/ml penicillin, and 10 µg/ml streptomycin in a 5% CO_2 incubator at 37°C.

For coimmunoprecipitation, $4x10^6$ HEK293 cells were plated onto two 10 cm petri dishes. Twenty-four hours later, cells were cotransfected with V5 tagged-RUND-1 and either GFP, GFP::RIC-19 or GFP::TBC-8 using TurboFect *in vitro* Transfection Reagent according to the manufacturer's protocol (Fermentas). After 24 hours, cells were washed with PBS and harvested in lysis buffer (50

mM Tris pH 7.5, 150 mM NaCl, 1% Triton X100, 0.5 mM EDTA, 10% glycerol, Complete Mini Protease inhibitor (Roche)) for 30 min at 4°C. Lysates were pre-cleared by centrifugation at 4°C and the supernatant was incubated with 2 µg monoclonal anti-GFP antibody (clone 3E6, Invitrogen) for three hours at 4°C. Protein G Plus-sepharose beads (Pierce) were added. After incubating for two hours, the beads were washed three times with washing buffer (50 mM Tris pH 7.5, 500 mM NaCl, 0.1% Triton X100, 0.5 mM EDTA, 10% glycerol, Complete Mini Protease inhibitor (Roche)) and resuspended in Laemmli loading buffer. Samples were resolved on 10% SDS-polyacrylamide gels and blotted onto a nitrocellulose membrane. To detect coprecipitated proteins, we added a mixture of two mouse monoclonal anti-GFP antibodies (1:1000, clones 7.1 and 13.1, Roche) and monoclonal anti-V5 antibody (1:5000, Invitrogen) followed by goat anti-mouse horseradish peroxidase-conjugated secondary antibody (1:10,000, Jackson Laboratory). A FujiFilm LAS 3000 processor was used to develop images, which were then edited using ImageJ software (National Institutes of Health).

Fluorescence electron microscopy (fEM)

Correlative fEM was performed as previously described (Watanabe et al., 2011) with a slight modification in the protocol. In brief, transgenic animals expressing tdEos were high-pressure frozen and freeze-substituted in 0.1% potassium permanganate (EMS) + 0.001% osmium tetroxide (EMS) in 95% acetone (EMS). The freeze-substitution protocol was as follows: -90ºC for 30 hours, 5ºC/hour to -50ºC, -50ºC for 2 hours, and 5ºC/hour to -30ºC. The fixatives were removed at -50ºC, and a solution containing 0.1% uranyl acetate (Polysciences) was added to the specimens. The uranyl acetate solution was removed when the temperature reached -30ºC. The animals were then embedded into GMA plastic (SPI). Eighty nm thick sections were sliced and mounted onto a pre-cleaned coverglass. The PALM imaging was performed using the Zeiss PAL-M (Zeiss, Prototype Serial No. 2701000005) following the application of gold fiduciary markers (100nm; microspheres-nanospheres.com). The same sections were imaged using a backscatter electron detector on scanning electron microscope (FEI Nova Nano). The PALM and electron micrographs were aligned based on the fiduciary markers in Photoshop (Adobe Photoshop CS5). For the purpose of presentation, we applied a gradient transparency to the PALM image - only the background black pixels are transparent.

Electron microscopy of synaptic and dense-core vesicles

High pressure freeze electron microscopy and analysis of synaptic profiles were performed as described (Rostaing et al., 2004; Sumakovic et al., 2009).

Electrophysiology

Young adult hermaphrodites were used for electrophysiological analysis as described (Liu et al., 2009). In brief, animals were immobilized on a Sylgard-coated glass coverslip by applying a cyanoacrylate adhesive along the dorsal side. A longitudinal incision was made in the dorsolateral region. The cuticle flap was folded back and glued to the coverslip, exposing the ventral nerve cord and two adjacent muscle quadrants. An upright microscope (Axioskop; Carl Zeiss, Inc.) equipped with a 40x water immersion lens and 15x eyepieces was used for viewing the preparation. All experiments were performed with the bath at room temperature using single electrode (borosilicate glass, R ~ 5 MΩ) voltage clamp (Heka, EPC-10) with two stage capacitive compensation optimized at rest, and series resistance compensated to 50%. Electrically evoked responses were elicited using an electrode with a tip resistance of approximately 3–5 MΩ positioned along the ventral nerve cord approximately one muscle cell body away from the patched muscle. A square wave depolarizing current of 0.5 ms at 25 V was delivered from an SIU5 stimulation isolation unit driven by an S48 stimulator (Grass Technologies). The standard pipette solution was (all concentrations in mM) [KCl 120; KOH 20; $MgCl_2$ 4; TES 5; $CaCl_2$ 0.25; EGTA 5; Na_2ATP 4; sucrose 36] and the standard extracellular solution was [NaCl 150; KCl 5; $CaCl_2$ 5; $MgCl_2$ 1; sucrose 5; HEPES 15; glucose 10]. Experiments were controlled using PatchMaster software (Heka). Analog data were digitized at 10 kHz and filtered at 2 kHz.

List of strains

CB4856 Hawaiian wild-isolate
EG281 *rund-1(ox281) X*
EG328 *rund-1(ox328) X*
EG334 *cccp-1(ox334) III*
EG1285 *oxIs12[Punc-47:GFP, lin-15+] X lin-15(n765ts) X*
EG3404 *unc-31(e928) IV*
EG3654 *egl-30(tg26) I ; cccp-1(ox334) III*
EG3738 *gsa-1(ce81) I ; unc-31(e928) IV*
EG3741 *rund-1(ox281) X dpy-3(e27) X*
EG3765 *egl-30(tg26) I ; rund-1(ox281) X*
EG3773 *egl-30(tg26) I ; unc-2(e55) X*
EG3774 *egl-30(tg26) I ; unc-18(md299) X*
EG3775 *egl-30(tg26) I ; unc-68(e540) V*
EG3782 *egl-30(tg26) I ; egl-3(ok979) V*
EG3797 *egl-30(tg26) I ; rund-1(ox328) X*
EG4033 *egl-30(tg26) I ; unc-104(e1265) II*
EG4044 *egl-30(tg26) I ; unc-68(r1162) V*
EG4045 *unc-31(e928) IV ; rund-1(ox281) X*
EG4167 *rund-1(ox281) X ; oxEx779[T19D7, Pmyo-2::gfp]*
EG4248 *rund-1(ox281) X oxIs12[Punc-47:GFP, lin-15+] X*
EG4322 *ttTi5605 II ; unc-119(ed9) III*
EG4358 *cccp-1(ox334) III ; oxEx1113[RPCI94_09N13, Pmyo-2::gfp, lin-15(+)]*
EG4532 *egl-30(tg26) I*
EG4780 *cccp-1(e1122) III*
EG4781 *egl-30(tg26) I ; cccp-1(e1122) III*
EG4815 *gsa-1(ce81) I ; rund-1(ox281) X*
EG4816 *gsa-1(ce81) I ; rund-1(ox328) X*
EG4923 *lin-15(n765ts) X ; oxEx1134[Prund-1::GFP, lin-15(+)]*
EG4937 *rab-2(n501) I ; rund-1(ox281) X*
EG4938 *rab-2(n777) I ; rund-1(ox281) X*
EG4939 *egl-30(tg26) I rab-2(n501) I*
EG4940 *egl-30(tg26) I rab-2(n777) I*
EG4941 *rab-2(n501) I*
EG5003 *unc-119(ed9) III ; cxTi10882 IV*
EG5039 *rab-2(n3263) I ; rund-1(ox281) X*
EG5102 *egl-4(ks62) IV ; rund-1(ox281) X*
EG5103 *egl-4(ks62) IV ; rund-1(ox328) X*
EG5108 *ceh-17(np1) I ; rund-1(ox281) X*
EG5109 *ceh-17(np1) I ; rund-1(ox328) X*
EG5111 *rab-2(n3263) I ; rund-1(ox328) X*
EG5112 *rab-2(n3263) I ; egl-4(ks62) IV*
EG5170 *egl-4(ks62) IV*
EG5228 *nuIs183[Punc-129::NLP-21-Venus, Pmyo-2::GFP] III ; rund-1(ox281) X*
EG5231 *nuIs183[Punc-129::NLP-21-Venus, Pmyo-2::GFP] III ; rund-1(ox328) X*
EG5232 *rab-2(n3263) I ; nuIs183[Punc-129::NLP-21-Venus, Pmyo-2::GFP] III*
EG5258 *nuIs183[Punc-129::NLP-21-Venus, Pmyo-2::GFP] III cccp-1(ox334) III*
EG5260 *ceIs61[Punc-129::flp-3::venus, Punc-129::mCherry-snb-1, Pttx-3::mCherry] II ; rund-1(ox281) X*
EG5261 *ceIs61[Punc-129::flp-3::venus, Punc-129::mCherry-snb-1, Pttx-3::mCherry] II ; rund-1(ox328) X*
EG5334 *ceIs61[Punc-129::flp-3::venus, Punc-129::mCherry-snb-1, Pttx-3::mCherry] II ; cccp-1(ox334) III*
EG5340 *rab-2(nu415) I ; rund-1(ox281) X*
EG5341 *rab-2(nu415) I ; rund-1(ox328) X*
EG5348 *cccp-1(ox334) III ; rund-1(ox281) X*

EG5349 *cccp-1(ox334) III ; rund-1(ox328) X*
EG5505 *rund-1(tm3622) X*
EG5606 *oxIs590[Cb unc-119(+), Prund-1::rund-1(+)::tagRFP] II ; unc-119(ed9) III*
EG5608 *oxIs592[Cb unc-119(+), Prund-1::rund-1(+)::eGFP] II ; unc-119(ed9) III*
EG5609 *egl-30(tg26) I ; rund-1(tm3622) X*
EG5610 *egl-30(tg26) I rab-2(nu415) I*
EG5627 *rab-2(nu415) I*
EG5631 *oxIs590[Cb unc-119(+), Prund-1::rund-1(+)::tagRFP] II ; rund-1(tm3622) X*
EG5633 *oxIs592[Cb unc-119(+), Prund-1::rund-1(+)::eGFP] II ; rund-1(tm3622) X*
EG5635 *ceIs61[Punc-129::flp-3::venus, Punc-129::mCherry-snb-1, Pttx-3::mCherry] II ; rund-1(tm3622) X*
EG5636 *ceIs61[Punc-129::flp-3::venus, Punc-129::mCherry-snb-1, Pttx-3::mCherry] II ; egl-3(ok979) V ; rund-1(tm3622) X*
EG5644 *cccp-1(ox334) III ; egl-3(ok979) V*
EG5645 *egl-3(ok979) V ; rund-1(tm3622) X*
EG5647 *rab-2(nu415) I ; egl-3(ok979) V*
EG5648 *rab-2(nu415) I ; rund-1(tm3622) X*
EG5649 *rab-2(nu415) I ; cccp-1(ox334) III*
EG5674 *nuIs183[Punc-129::NLP-21-Venus, Pmyo-2::GFP] III ; rund-1(tm3622) X*
EG5745 *unc-119(ed9) III ; oxSi13[Prund-1::aman-2::eGFP, Cbunc-119] IV*
EG5748 *unc-119(ed9) III ; oxSi59[Prund-1::eGFP::tram-1, Cbunc-119] IV*
EG5805 *oxSi95[Prund-1::rund-1(+)::tdEos, Cb-unc-119] II ; unc-119(ed9) III*
EG5849 *oxSi95[Prund-1::rund-1(+)::tdEos, Cb-unc-119] II ; rund-1(tm3622) X*
EG5857 *egl-30(tg26) I ; unc-50(e306) III*
EG5858 *egl-30(tg26) I unc-74(ox78) I*
EG5859 *oxIs590[Cb unc-119(+), Prund-1::rund-1(+)::tagRFP] II ; oxSi13[Prund-1::aman-2::eGFP, Cbunc-119] IV*
EG5860 *oxIs590[Cb unc-119(+), Prund-1::rund-1(+)::tagRFP] II ; oxSi59[Prund-1::eGFP::tram-1, Cbunc-119] IV*
EG5912 *cccp-1(ox334) III ; nuIs195[Punc-129::ins-22::venus, Pmyo-2::gfp]*
EG5913 *nuIs195[Punc-129::ins-22::venus, Pmyo-2::gfp] ; rund-1(tm3622) X*
EG5914 *cccp-1(ox334) III ; ceIs72[Punc-129::ida-1::GFP, Pttx-3::mCherry]*
EG5915 *ceIs72[Punc-129::ida-1::GFP, Pttx-3::mCherry] ; rund-1(tm3622) X*
EG5936 *rab-2(nu415) I ; ceIs72[Punc-129::ida-1::GFP, Pttx-3::mCherry]*
EG5938 *rab-2(nu415) I ; nuIs195[Punc-129::ins-22::venus, Pmyo-2::gfp]*
EG6010 *ric-19(pk690) I ; rund-1(tm3622) X*
EG6193 *unc-119(ed9) III ; oxSi266[Prund-1::eGFP::rab-5, Cb unc-119] IV*
EG6244 *nuIs183[Punc-129::NLP-21-Venus, Pmyo-2::GFP] III ; egl-3(ok979) V ; rund-1(tm3622) X*
EG6286 *rab-2(nu415) I ; nuIs183[Punc-129::NLP-21-Venus, Pmyo-2::GFP] III ; rund-1(tm3622) X*
EG6359 *unc-119(ed9) III ; oxSi308[Prund-1::eGFP::rab-6.2, Cb-unc-119] IV*
EG6361 *unc-119(ed9) III ; oxSi310[Prund-1::eGFP::rab-7, Cb-unc-119] IV*
EG6362 *unc-119(ed9) III ; oxSi311[Prund-1::eGFP::rab-11.1, Cb-unc-119] IV*
EG6363 *unc-119(ed9) III ; oxSi312[Prund-1::eGFP::e-COP, Cb-unc-119] IV*
EG6364 *unc-119(ed9) III ; oxSi313[Prund-1::eGFP::syn-13, Cb-unc-119] IV*
EG6365 *unc-119(ed9) III ; oxSi314[Prab-2::eGFP::rab-2, Cb-unc-119] IV*
EG6366 *unc-119(ed9) III ; oxSi315[Prund-1::eGFP::syx-6, Cb-unc-119] IV*
EG6368 *rab-2(nu415) I ; oxSi314[Prab-2::eGFP::rab-2, Cb-unc-119] IV*
EG6369 *oxIs590[Cb unc-119(+), Prund-1::rund-1(+)::tagRFP] II ; oxSi266[Prund-1::eGFP::rab-5, Cb unc-119]* IV
EG6371 *oxIs590[Cb unc-119(+), Prund-1::rund-1(+)::tagRFP] II ; oxSi308[Prund-1::eGFP::rab-6.2, Cb-unc-119] IV*
EG6373 *oxIs590[Cb unc-119(+), Prund-1::rund-1(+)::tagRFP] II ; oxSi310[Prund-1::eGFP::rab-7, Cb-unc-119]* IV
EG6374 *oxIs590[Cb unc-119(+), Prund-1::rund-1(+)::tagRFP] II ; oxSi311[Prund-1::eGFP::rab-11.1, Cb-unc-119] IV*

EG6375 *oxIs590[Cb unc-119(+), Prund-1::rund-1(+)::tagRFP] II ; oxSi312[Prund-1::eGFP::e-COP, Cb-unc*-119] IV
EG6376 *oxIs590[Cb unc-119(+), Prund-1::rund-1(+)::tagRFP] II ; oxSi313[Prund-1::eGFP::syn-13, Cb-unc-119]* IV
EG6377 *oxIs590[Cb unc-119(+), Prund-1::rund-1(+)::tagRFP] II ; oxSi314[Prab-2::eGFP::rab-2, Cb-unc-119] IV*
EG6378 *oxIs590[Cb unc-119(+), Prund-1::rund-1(+)::tagRFP] II ; oxSi315[Prund-1::eGFP::syx-6, Cb-unc-119] IV*
EG6383 *oxSi314[Prab-2::eGFP::rab-2, Cb-unc-119] IV ; rund-1(ox281) X*
EG6384 *oxSi314[Prab-2::eGFP::rab-2, Cb-unc-119] IV ; rund-1(tm3622) X*
EG6388 *nuIs183[Punc-129::NLP-21-Venus, Pmyo-2::GFP] III ; rund-1(tm3622) X ; oxEx1520[Punc-129::rund-1::tagRFP, Pmyo-2::mCherry]*
EG6389 *rund-1(tm3622) X ; oxEx1521[Prund-1::RUNDC1 cDNA::tagRFP, Pmyo-2::gfp]*
EG6390 *rund-1(ox281) X ; oxEx1522[Prund-1::RUNDC1 cDNA::tagRFP, Pmyo-2::gfp]*
EG6391 *rund-1(tm3622) X ; oxEx1523[Phsp16.2::rund-1 cDNA::tagRFP, Pmyo-2::gfp]*
EG6652 *rund-1(tm3622) X ; oxEx1575[Prund-1::rund-1(+)::tdEos, Pmyo-2::gfp]*
EG6917 *oxIs590[Cb unc-119(+), Prund-1::rund-1(+)::tagRFP] II ; cccp-1(ox334) III*
EG6920 *cccp-1(ox334) III ; oxSi314[Prab-2::eGFP::rab-2, Cb-unc-119] IV*
EG6922 *oxSi315[Prund-1::eGFP::syx-6, Cb-unc-119] IV ; rund-1(tm3622) X*
EG6923 *oxSi308[Prund-1::eGFP::rab-6.2, Cb-unc-119] IV ; rund-1(tm3622) X*
EG6927 *rab-2(nu415) I ; oxIs590[Cb unc-119(+), Prund-1::rund-1(+)::tagRFP] II*
EG6929 *oxSi503[Prund-1::rund-1 CC::tagRFP, Cb-unc-119] II ; unc-119(ed9) III*
EG6933 *rund-1(tm3622) X ; oxEx1366[Cb-unc-119(+) cccp-1::eGFP, Pmyo-2::mCherry, Pmyo-3::mCherry, Prab-3::mCherry]*
EG6934 *rab-2(nu415) I ; oxEx1366[Cb-unc-119(+) cccp-1::eGFP, Pmyo-2::mCherry, Pmyo-3::mCherry, Prab-3::mCherry]*
EG6941 *oxSi503[Prund-1::rund-1 CC::tagRFP, Cb-unc-119] II ; rund-1(tm3622) X*
EG6943 *oxSi505[Prund-1::rund-1 RUN::tagRFP, Cb-unc-119] II ; unc-119(ed9) III*
EG6945 *oxSi505[Prund-1::rund-1 RUN::tagRFP, Cb-unc-119] II ; rund-1(tm3622) X*
EG6949 *cccp-1(ox334) III ; oxEx1622[Prab-3::cccp-1::gfp, Prund-1::rund-1::tagRFP]*
EG6951 *cccp-1(ox334) III ; oxEx1624[Prab-3::cccp-1::gfp, Prab-3::tagRFP::rab-2(DA)]*
EG6953 *cccp-1(ox334) III ; oxEx1626[Prab-3::cccp-1::gfp, Prab-3::tagRFP::rab-2(DN)]*
EG6982 *cccp-1(ox334) III ; oxEx1628[Prab-3::cccp-1::gfp, Punc-122::gfp]*
EG7187 *unc-119(ed9) III ; oxEx1366[Cb-unc-119(+) cccp-1::eGFP, Pmyo-2::mCherry, Pmyo-3::mCherry, Prab-3::mCherry]*
EG7227 *lin-15(n765ts) X ; oxEx1251[Pcccp-1::gfp, lin-15(+)]*
EG7242 *rund-1(ox281) X lin-15(n765ts) X ; oxEx1197[Prab-3::rund-1 cDNA::mCherry, lin-15(+)]*
EG7244 *rund-1(ox281) X lin-15(n765ts) X ; oxEx1260[Pvha-6::rund-1 cDNA::mCherry, lin-15(+)]*
EG7249 *eri-1(mg366) IV ; lin-15(n744) X*
FK234 *egl-4(ks62) IV*
IB16 *ceh-17(np1) I*
GQ640 *ric-19(ok833) I ; nuIs183[Punc-129::NLP-21-Venus, Pmyo-2::GFP] III*
GQ641 *tbc-8(tm3802) III nuIs183[Punc-129::NLP-21-Venus, Pmyo-2::GFP] III*
GQ693 *nuIs183[Punc-129::NLP-21-Venus, Pmyo-2::GFP] III ; rund-1(tm3622) X*
GQ698 *ric-19(ok833) I ; nuIs183[Punc-129::NLP-21-Venus, Pmyo-2::GFP] III ; rund-1(tm3622) X*
GQ699 *tbc-8(tm3802) III nuIs183[Punc-129::NLP-21-Venus, Pmyo-2::GFP] III ; rund-1(tm3622) X*
KG421 *gsa-1(ce81) I*
KG1395 *nuIs183[Punc-129::NLP-21-Venus, Pmyo-2::GFP] III*
KG1475 *rab-2(ce365) I ; nuIs183[Punc-129::NLP-21-Venus, Pmyo-2::GFP] III*
KG1624 *nuIs195[Punc-129::ins-22::venus, Pmyo-2::gfp]*
KG1645 *ceIs61[Punc-129::flp-3::venus, Punc-129::mCherry-snb-1, Pttx-3::mCherry] II*
KG1655 *rab-2(ce365) I ; ceIs61[Punc-129::flp-3::venus, Punc-129::mCherry-snb-1, Pttx-3::mCherry] II*
KG1852 *ceIs72[Punc-129::ida-1::GFP, Pttx-3::mCherry]*
MT1093 *rab-2(n501) I*
MT1656 *rab-2(n777) I*
N2 Bristol wild-isolate, standard lab wild type

NL2003 *ric-19(pk690) I*
VC671 *egl-3(ok979) V*
XZ1022 *rab-2(nu415) I; oxIs590[Cb unc-119(+), Prund-1::rund-1(+)::tagRFP] II ; oxSi266[Prund-1::eGFP::rab-5, Cb unc-119]* IV
XZ1023 *rab-2(nu415) I; oxIs590[Cb unc-119(+), Prund-1::rund-1(+)::tagRFP] II ; oxSi308[Prund-1::eGFP::rab-6.2, Cb-unc-119] IV*
XZ1024 *rab-2(nu415) I; oxIs590[Cb unc-119(+), Prund-1::rund-1(+)::tagRFP] II ; oxSi310[Prund-1::eGFP::rab-7, Cb-unc-119]* IV
XZ1026 *rab-2(nu415) I; nuIs183[Punc-129::NLP-21-Venus, Pmyo-2::GFP] III*
XZ1027 *nuIs183[Punc-129::NLP-21-Venus, Pmyo-2::GFP] III cccp-1(ox334) III; rund-1(tm3622)*
XZ1028 *rab-2(nu415); nuIs183[Punc-129::NLP-21-Venus, Pmyo-2::GFP] III cccp-1(ox334) III*
ZH382 *rab-2(n3263) I*

List of plasmids

Miscellaneous plasmids

RPCI94_09N13	BAC carrying the *C. briggsae* ortholog of *cccp-1*, used to make *oxEx1113* (10 ng/μl)
T19D7	cosmid carrying the *rund-1* gene T19D7.4, used to make *oxEx779* (10 ng/μl)
yk471g7	*rund-1* full length cDNA
yk530g8	*cccp-1b* full length cDNA
Prab-3::tagRFP::rab-2(DA) used to make oxEx1624 (5 ng/μl)	
Prab-3::tagRFP::rab-2(DN) used to make oxEx1626 (5 ng/μl)	

Gateway destination vectors

pCFJ150	Gateway destination vector for insertion at chromosome II Mos site *ttTi5605*
pCFJ201	Gateway destination vector for insertion at chromosome IV Mos site *cxTi10882*
pDEST-R4-R3	Gateway destination vector

Gateway entry clones

pCM1.56	*Phsp-16.2* [4-1] (493 bp of the *hsp-16.2* promoter upstream of the ATG)
pCR110	*GFP* [1-2]
pENTR[4-1] P[rab-3]	*Prab-3* [4-1] (1224 bp of the *rab-3* promoter upstream of and including the ATG)
pGH107	*tagRFP::let-858* 3'UTR [2-3]
pGH112	*eGFP::let-858* 3'UTR [2-3]
pGH115	*eGFP* [1-2]
pGH271	*tdEos::let-858* 3'UTR [2-3]
pMA15	*Pcccp-1* [4-1] (1696 bp of the *cccp-1* promoter upstream of and including the ATG)
pMA18	*cccp-1b* cDNA [1-2] (from yk530g8)
pMA20	*rund-1* cDNA [1-2] (from yk471g7)
pMA108	*rab-5* cDNA::let-858 3'UTR [2-3]
pMA115	*rab-7* cDNA::let-858 3'UTR [2-3]
pMA116	*rab-11.1* cDNA::let-858 3'UTR [2-3]
pMA132	*rab-6.2* cDNA::let-858 3'UTR [2-3]
pMA145	*syx-6* cDNA::let-858 3'UTR [2-3]
pMA157	RUNDC1 cDNA[1-2]
pMA165	*rund-1* coiled-coil domain [1-2] (aa 1-261)
pMA166	*rund-1* RUN domain [1-2] (aa 262-549)
pPM1	*aman-2* [1-2]
pPM2	*tram-1* [2-3]
pSD11	*Prab-2* [4-1] (3237 bp of the *rab-2* promoter upstream of the ATG)
pSD12	*Punc-129* [4-1] (2645 bp of the *unc-129* promoter upstream of the ATG)
pSD16	*rab-2*(+) gene with introns and *rab-2* 3'UTR [2-3]
pSD25	*syn-13* with *let-858* 3'UTR [2-3]
pSD26	ε-COP with let-858 3'UTR [2-3]
pT19D7.4 [4-1]	*Prund-1* [4-1] (2733 bp of the *rund-1* promoter upstream of and including the ATG)

pT19D7.4 [1-2] *rund-1(+)* gene with introns [1-2]
p_VW02B12L.1_93 *Pvha-6* [4-1] (881 bp of the *vha-6* promoter upstream of and including the ATG)

Gateway expression constructs

pAP4	*Prund-1::gfp*	used to make *oxEx1134* (10 ng/μl)
pMA17	*Pcccp-1::gfp*	used to make *oxEx1251* (10 ng/μl)
pMA24	*Prab-3::rund-1* cDNA::mCherry	used to make *oxEx1197* (10 ng/μl)
pMA38	*Pvha-6::rund-1* cDNA::mCherry	used to make *oxEx1260* (10 ng/μl)
pMA56	*Prund-1::rund-1(+)::tagRFP*	used to make *oxIs590* and *oxEx1622* (10 ng/μl)
pMA57	*Prund-1::rund-1(+)::eGFP*	used to make *oxIs592*
pMA58	*Pcccp-1::cccp-1 cDNA::eGFP*	used to make *oxEx1366* (50 ng/ml)
pMA74	*Prund-1::aman-2::eGFP*	used to make *oxSi13*
pMA75	*Prund-1::eGFP::tram-1*	used to make *oxSi59*
pMA90	*Prund-1::rund-1(+)::tdEos*	used to make *oxEx1575* (10 ng/μl) & *oxSi95*
pMA112	*Prund-1::eGFP::rab-5*	used to make *oxSi266*
pMA118	*Prund-1::eGFP::rab-7*	used to make *oxSi310*
pMA119	*Prund-1::eGFP::rab-11.1*	used to make *oxSi311*
pMA138	*Prund-1::eGFP::rab-6.2*	used to make *oxSi308*
pMA147	*Prund-1::eGFP::syx-6*	used to make *oxSi315*
pMA150	*Phsp16.2::rund-1 cDNA::tagRFP*	used to make *oxEx1523* (10 ng/μl)
pMA152	*Punc-129::rund-1 cDNA::tagRFP*	used to make *oxEx1520* (10 ng/μl)
pMA159	*Prab-3::cccp-1 cDNA::eGFP*	used to make *oxEx1622, oxEx1624, oxEx1626, oxEx1628* (10 ng/μl)
pMA161	*Prund-1::RUNDC1 cDNA::tagRFP*	used to make *oxEx1521 & oxEx1522* (10 ng/μl)
pMA172	*Prund-1::rund-1 CC::tag RFP*	used to make *oxSi503*
pMA173	*Prund-1::rund-1 RUN::tagRFP*	used to make *oxSi505*
pSD18	*Prab-2::eGFP::rab-2(+)*	used to make *oxSi314*
pSD30	*Prund-1::eGFP::syn-13*	used to make *oxSi313*
pSD31	*Prund-1::eGFP::ε-COP*	used to make *oxSi312*

Supplemental References

Edgar, R.C. (2004). MUSCLE: multiple sequence alignment with high accuracy and high throughput. Nucleic Acids Res *32*, 1792–1797.

Frøkjaer-Jensen, C., Davis, M.W., Hopkins, C.E., Newman, B.J., Thummel, J.M., Olesen, S.-P., Grunnet, M., and Jorgensen, E.M. (2008). Single-copy insertion of transgenes in Caenorhabditis elegans. Nat. Genet *40*, 1375–1383.

Liu, Q., Hollopeter, G., and Jorgensen, E.M. (2009). Graded synaptic transmission at the Caenorhabditis elegans neuromuscular junction. Proc. Natl. Acad. Sci. U.S.A. *106*, 10823–10828.

Mello, C.C., Kramer, J.M., Stinchcomb, D., and Ambros, V. (1991). Efficient gene transfer in C.elegans: extrachromosomal maintenance and integration of transforming sequences. EMBO J *10*, 3959–3970.

Rostaing, P., Weimer, R.M., Jorgensen, E.M., Triller, A., and Bessereau, J.-L. (2004). Preservation of immunoreactivity and fine structure of adult C. elegans tissues using high-pressure freezing. J. Histochem. Cytochem *52*, 1–12.

Watanabe, S., Punge, A., Hollopeter, G., Willig, K.I., Hobson, R.J., Davis, M.W., Hell, S.W., and Jorgensen, E.M. (2011). Protein localization in electron micrographs using fluorescence nanoscopy. Nat. Methods *8*, 80–84.